www.sciencemag.org/cgi/content/full/science.1230374 /DC1

# Supplementary Materials for

## Topology of Feather Melanocyte Progenitor Niche Allows Complex Pigment Patterns to Emerge

S. J. Lin, J. Foley, T. X. Jiang, C. Y. Yeh, P. Wu, A. Foley, C. M. Yen, Y. C. Huang, H. C. Cheng, C. F. Chen, B. Reeder, S. H. Jee, R. B. Widelitz, C. M. Chuong*

*Corresponding author. E-mail: cmchuong@usc.edu

Published 25 April 2013 on *Science* Express
DOI: 10.1126/science.1230374

**This PDF file includes:**

## Materials and Methods

### Animals

Chicken breeds with distinct plumage color patterns based on different genetic backgrounds were used (*29-30*). Barred Plymouth Rock chickens, Rode Island Red chickens and Silver Sebright chickens were purchased from Belt Hatchery (Fresno, CA, USA); Silver Laced Wyandotte chickens, Silver Spangled Hamburg chickens, Delaware chickens, and Speckled Sussex chickens were from Welp Hatchery (Bancroft, IA, USA); Black-feathered Taiwan Country chickens and feather follicle specimens of Helmeted Guineafowls (*Numida meleagris*) and pigeons (*Columba livia*) were provided by coauthor C. F. C. from Department of Animal Science, College of Agriculture and Natural Resources, National Chung Hsing University, Taichung, Taiwan. Black-feathered Taiwan Country chickens have been described (fig. S2C) (*31*). Birds were kept and fed *ad lib* in our animal facilities. For invasive experimental procedures, birds were anesthetized with 10 mg/kg (body weight) of ketamine and xylocaine (2:1).

### BrdU tracing

For BrdU tracing, the flight feathers of 4 to 6-month-old chickens were plucked. In our breeds, the regenerating flight feathers emerged from the follicle to the skin surface about 14 days after plucking and the period for the growing phase was about 9 weeks. To investigate melanocyte cell dynamics at different stages of growth, adjacent feathers were plucked 14 days apart (day 0, day 14, day 28) and the chickens were labeled by intramuscular injection of BrdU (Sigma-Aldrich, St. Louis, MO) at 10mg per kg (body weight) every 12 hours for 14 days (day 28 to day 42) and chased for up to 2 weeks. The birds were then sacrificed 0, 2, 4, 6, 8, 10, and 14 days after tracing and the feather follicle samples were collected. In this way, flight feathers at different periods of the growing phase were labeled and traced: feathers were labeled in the early (0-14 days after plucking), middle (15-28 days after plucking) and late (29-42 days after plucking) period of the growing phase.

### DiI labeling and protein-coated bead implantation

DiI (Molecular Probes) and protein coated beads (ASIP, OriGene, Rockville, MD, USA) were prepared and injected as described (*32*). Briefly, under anesthesia, DiI was injected through the regenerating follicle wall at the level of the lower bulge of 4 to 6-month-old chickens. ASIP-coated beads were injected through the feather wall into the feather pulp adjacent to the feather epithelium at the level of the middle to upper collar region. Follicles were collected at desired time points and photographed. The samples were further processed for immunostaining or section *in situ* hybridization.

### Transplantation of papilla ectoderm to chicken embryos

The transplantation was performed as we previously described (*9*). White Leghorn chicken embryos were used as a host, because their genetic defect caused a deletion of cutaneous melanocytes and the developing feather buds and post-natal feathers lacked pigment. The papilla ectoderm region was carefully microdissected from the resting follicles of pigmented feathers in quails and transplanted to the hind limb bud of E3 White Leghorn chicken embryos. The pigmentation of the feather buds in the transplanted region was photographed after 5 days of incubation and the embryo

specimens were collected for immunohistochemical analysis for the presence of melanocytes in the pigmented feather buds.

Histology and immunostaining

The collected feather follicle samples were fixed in 4% paraformaldehyde in phosphate buffered saline (PBS) over night, and then serially dehydrated with alcohol and embedded in paraffin. For cryostat, the samples were fixed in 1% paraformaldehyde in PBS overnight and embedded in OCT. Paraffin sections (7μm) or cryosections (8-10μm) were stained with hematoxylin and eosin or prepared for immunostaining following routine procedures (*33*). The following antibodies were used: mouse anti-Mitf (1:200, C3 and C5, Abcam), mouse anti-MART-1 (1:200, Thermo Scientific), mouse anti-PCNA (1:200, Chemicon), rat anti-BrdU (1:200, Abcam), QCPN antibody (a quail cell marker, Developmental Studies Hybridoma Bank), Alexa Fluor® 594 anti-mouse IgG1(γ1) (1:200, Invitrogen), Alexa Fluor® 488 anti-mouse IgG2b (1:200, Invitrogen), Alexa Fluor® 488 anti-mouse IgG2a (1:200, Invitrogen), Alexa Fluor® 594 anti-mouse IgG2a (1:200, Invitrogen), Texas Red donkey anti-rat IgG (1:200, Jackson ImmunoResearch), DyLight 488 donkey anti-mouse IgG (1:200, Jackson ImmunoResearch). Paraffin (7μm) and cryostat sections (8-10μm) were prepared for staining. Antigen retrieval was performed according to the suggestions from the antibody manufacturers. The specimens were blocked with 5% bovine serum albumin (Sigma) in PBS for 1 hour, incubated in primary antibodies in 1% albumin/PBS over night at 4$^{o}$C, and rinsed with PBS extensively. For immunohistochemistry, color was developed with AEC peroxidase substrate kit (Vector Laboratories). To remove melanin color, the specimens were then bleached with $H_2O_2$ solution as described (*34*), and counter-stained with hematoxylin. For immunofluorescent staining, the specimens were incubated in secondary antibodies for 2 hours at room temperature. After being rinsed with PBS, the specimens were stained with nuclear dye DAPI (300nM in PBS, Sigma) for 10 min at room temperature and rinsed with PBS extensively before mounting with 50% glycerol in PBS. TUNEL staining was performed by use of a kit (Roche). Tyrosinase activity was determined in cryosections by tyramide reaction (Tyramide Signal Amplification Systems, PerkinElmer) as described (*35*).

*In situ* hybridization

Digoxigenin-labeled probes against chicken tyrosinase related protein-1 (TRP1) (nucleotides 511-1055; NM_205045.1), tyrosinase (TYR) (nucleotides 680-1154; NM_204160.1), and agouti signaling protein (ASIP) (nucleotides 52-453; NM_001115079.1) were synthesized by use of a digoxigenin RNA labeling kit according to the instructions from the manufacturer (DIG RNA Labeling kit, Roche) as described (*36*). To detect three-dimensional ASIP expression in feather mesenchyme, the epithelium of a growing feather was removed and the mesenchymal cylinder containing feather pulp and dermal papilla were further prepared for whole mount *in situ* hybridization. Paraffin sections and whole mount samples were prepared for *in situ* hybridization following routine procedures (*36*). To remove the melanin color, the sections were then bleached with $H_2O_2$ solution before being counterstained with eosin.

Three-dimensional reconstruction

Serial horizontal 7μm-sections of growing breast feather follicles from Barred Plymouth Rock chickens were first stained for Mitf. Microscopic images of the serial sections were taken and the serial images were aligned by software ImageJ 1.36b (National Institutes of Health, Bethesda, Maryland, USA). The distribution of melanocytes in the feather follicle was reconstructed using the software Amira (Visage Imaging, San Diego, CA, USA). The images were rendered as a three-dimensional view of melanocyte distribution in the feather follicle.

Explant culture and melanocyte culture

Feather melanocytes were cultured as described (*37*). Briefly, feather follicles were isolated and cut into explants containing the desired epithelial portion connected with the adjacent feather pulp. The feather explants with the pulp at the base of 6-well culture plates (BD Biosciences) were cultured in F12 medium (Invitrogen) containing 10% (v/v) fetal bovine serum (Gemini Bio-Products) and 1-fold concentrated Antibiotic-Antimycotic (Gibco) at 37$^{o}$C in an atmosphere of 95% air/5% $CO_2$. Culture medium was changed twice a week. After 70% confluency was reached, the explants were removed and cells were detached by 0.05% trypsin/EDTA (Gibco) immediately before they were used in the following experiments. Immunostaining showed that more than 97% of the outgrowing cells were positive for the MART-1 melanocyte marker. To test the effect of α-melanocyte stimulating hormone (α-MSH) on melanocyte differentiation, freshly isolated feather explants containing the adjacent pulp or the expanded melanocytes were cultured in the presence of α-MSH (1.25μg/ml, 2.5 μg/ml, 5 μg/ml, and 10 μg/ml, Sigma) for 7 days. The explants and cells were photographed and tyrosinase activity was determined by tyramide reaction (Tyramide Signal Amplification Systems, PerkinElmer) as described (*35*).

Real-time PCR analysis

Each feather follicle specimen (either from a pigmented or apigmented region) containing the epithelium spanning from papilla ectoderm to 3mm above ramogenic zone and the attached adjacent mesenchyme (including the peripheral and central pulp) was carefully microdissected. The epithelium with the connected pulp mesenchyme was then processed for real-time PCR analysis. Total RNA extraction and real-time PCR were performed as we previously described using Power SYBR Green PCR Master Mix (Applied Biosystems, U.S.A.) and a PX2 thermal cycler (Thermo Scientific) (*38*). The sequences of primers specific for genes analyzed were as following: tyrosinase-related protein 1 (TRP1)( NM_205045.1) (5'-CGTGTGCTGTGTGAAAGTAT-3' and 5'-GGATTTCTACGGATGGGACC-3'), tyrosinase (TYR) (NM_204160.1)(5'-GGATGACAGAGAGGATTGGC-3' and 5'-CCTGAGAAGCCAAACTTGC-3'), solute carrier family 24, member 5 (SLC24A5)( NM_001038497.2)(5'-CACAGAGAACAGGACGGAT-3' and 5'-TTCCTCCATCCTTTCTCTCC-3'), agouti signaling protein (ASIP) (NM_001115079.1) (5'-TCCCAGAAAGTCAGCAGAA-3' and 5'-TTGAAGTTTGGCACGCAG-3'), actin (NM_205518.1)(5'-GCTATGAACTCCCTGATGGTC-3' and 5'-GGACTCCATACCCAAGAAAGA-3').

Statistics

Data are expressed as the mean ± standard error of the mean. Two-tailed Student's t test was performed for comparison among groups using SigmaPlot 10.0 (Systat Software, San Jose, CA, USA) software. P-values were considered significant when less than 0.05. Data were plotted using SigmaPlot or Microsoft Excel.

**References and Notes:**


1. C. M. Chuong, V. A. Randall, R. B. Widelitz, P. Wu, T. X. Jiang, *Physiology* **27**, 61 (2012).
2. G. E. Hill, K. J. McGraw, *Bird Coloration*. G. E. Hill, K. J. McGraw, Eds., (Harvard University Press, Cambridge, Massachusetts, 2006).
3. A. M. Lucas, P. R. Stettenheim, *Avian Anatomy: Integument. Agriculture Handbook 362: Agricultural Research Service*. (US Dept. Agrculture, Washington DC, 1972), vol. 2.
4. M. Yu *et al.*, *Int. J. Dev. Biol.* **48**, 181 (2004).
5. C. Darwin, *On the origins of species by means of natural slection*. (John Murray, London, 1859).
6. F. Zhang *et al.*, *Nature* **463**, 1075 (2010).
7. Q. Li *et al.*, *Science* **327**, 1369 (2010).
8. E. Dupin, N. M. Le Douarin, *Oncogene* **22**, 3016 (2003).
9. Z. Yue, T. X. Jiang, R. B. Widelitz, C. M. Chuong, *Nature* **438**, 1026 (2005).
10. E. K. Nishimura *et al.*, *Nature* **416**, 854 (2002).
11. P. Rabbani *et al.*, *Cell* **145**, 941 (2011).
12. P. Stettenheim, *Science* **333**, 939 (2011).
13. G. Montalenti, *J. Exp. Zool.* **69**, 77 (1934).
14. A. R. Hellstrom *et al.*, *Pigment Cell Melanoma Res.* **23**, 521 (2010).
15. G. S. Barsh, *Trends Genet.* **12**, 299 (1996).
16. M. M. Ollmann, M. L. Lamoreux, B. D. Wilson, G. S. Barsh, *Genes Dev.* **12**, 316 (1998).
17. S. E. Millar, M. W. Miller, M. E. Stevens, G. S. Barsh, *Development* **121**, 3223 (1995).
18. C. R. Linnen, E. P. Kingsley, J. D. Jensen, H. E. Hoekstra, *Science* **325**, 1095 (2009).
19. E. Aberdam *et al.*, *J. Biol. Chem.* **273**, 19560 (1998).
20. M. Manceau, V. S. Domingues, R. Mallarino, H. E. Hoekstra, *Science* **331**, 1062 (2011).
21. C. Yoshihara *et al.*, *Gen. Comp. Endocrinol.* **175**, 495 (2012).
22. Y. Yamaguchi, V. J. Hearing, *Biofactors* **35**, 193 (2009).

23. S. Kondo, T. Miura, *Science* **329**, 1616 (2010).

24. R. O. Prum, S. Williamson, *Proc. Biol. Sci.* **269**, 781 (2002).

25. F. Lillie, H. Wang, *Physiol. Zool.* **14**,103 (1941).

26. Y. Yamaguchi *et al., J. Cell. Biol.* **165**, 275 (2004).

27. C. M. Chuong, M. K. Richardson, *Int. J. Dev. Biol.* **53**, 653 (2009).

28. S. J. Lin *et al. Develop. Growth Differ.* **55**, 139 (2013).

29. G. Coquerelle, *Les poules : Diversité génétique visible*. (L'Institut National de la Recherche Agronomique, Paris, 2000).

30. B. Reeder, *An Introduction to Color Forms of the Domectic Fowl*. (AuthourHouse, Bloomington, Indiana, 2006).

31. C. H. Chao *et al., J. Chin. Soc. Anim. Sci.* **34**, 65 (2005).

32. Z. Yue, T. X. Jiang, R. B. Widelitz, C. M. Chuong, *Proc. Natl. Acad. Sci. U.S.A.* **103**, 951 (2006).

33. M. Yu, P. Wu, R. B. Widelitz, C. M. Chuong, *Nature* **420**, 308 (2002).

34. W. Korytowski, T. Sarna, *J. Biol. Chem.* **265**, 12410 (1990).

35. R. Han, H. P. Baden, J. L. Brissette, L. Weiner, *Pigment Cell Res.* **15**, 290 (2002).

36. C. S. Ng *et al., PLoS Genet.* **8**, e1002748 (2012).

37. R. R. Bowers, J. E. Gatlin, *In Vitro Cell. Dev. Biol.* **21**, 39 (1985).

38. C. M. Yen, C. C. Chan, S. J. Lin, *Biomaterials* **31**, 4341 (2010).

**Extended lists of acknowledgement**

We thank the Imaging Core of USC Research Center for Liver Diseases (P30DK048522) and 8th Core Laboratory of National Taiwan University Hospital for their support.

**Fig. S1**

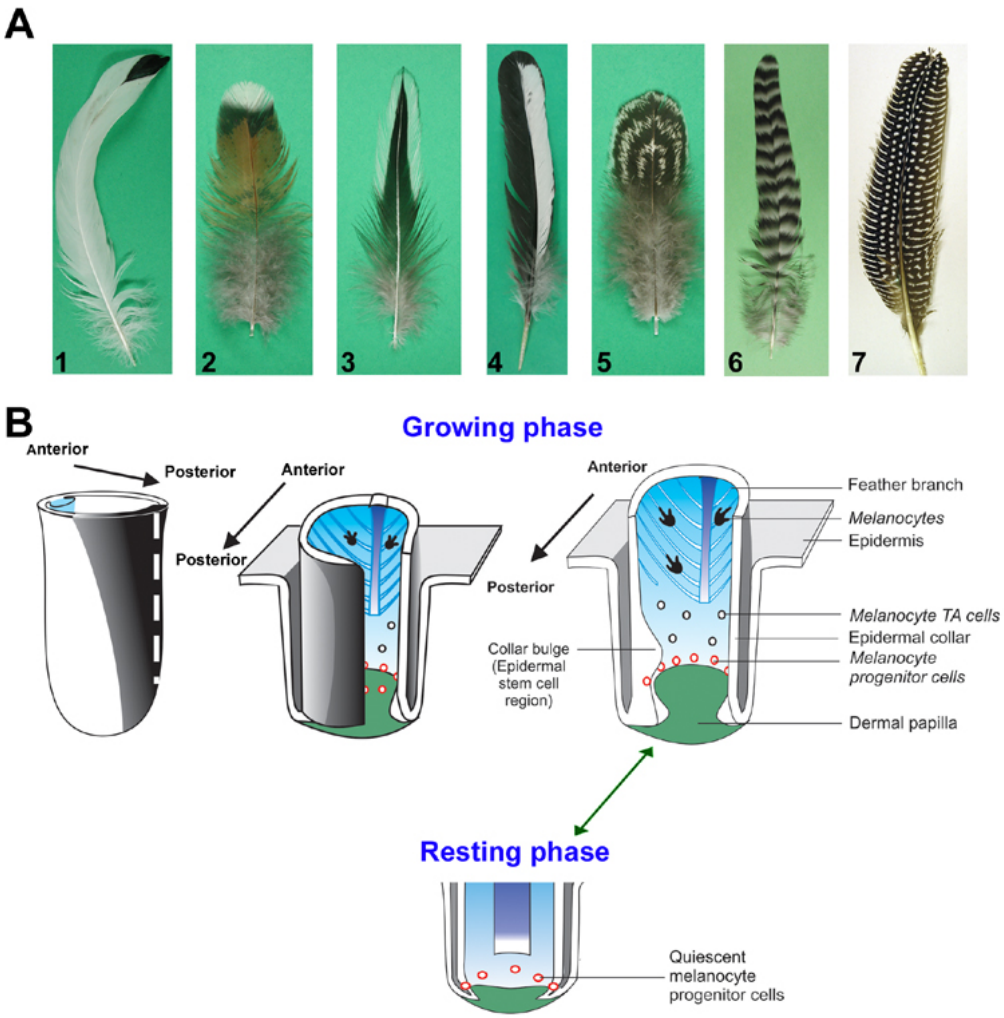


**Complexity of feather pigment patterns and feather follicle structure.**

A. Basic feather pigment patterns are shown here. (1) Distal black spangling. Sickle feather from a male Silver Spangled Hamburg chicken. (2) Distal white mottling. Breast feather from a female Speckled Sussex chicken. (3) Single peripheral lacing. Hackle feather from a male Silver Laced Wyandotte chicken. (4) Longitudinal stripe. Flight feather from a female Silver Laced Wyandotte chicken. (5) Multiple lacing. Breast feather from a female Dark Brahma chicken. (6) Horizontal barring. Sickle feather from a male Barred Plymouth Rock chicken. (7) Dots and stripes. Flight feather from a male Helmeted Guineafowl.

B. Schematic depictions of feather follicle structures in growing (upper panel) and resting (lower panel) phases. Dermal papilla is on the proximal end of the feather follicle. In the growing phase, feather keratinocytes proliferate to support elongation of the epithelial cylinder toward the distal end. When a growing feather gradually

emerges from skin, it opens from the posterior side (white dashed line) into a planar vane. In the resting phase, the feather follicle shrinks toward the proximal end. TA: transit amplifying.

**Fig. S2**

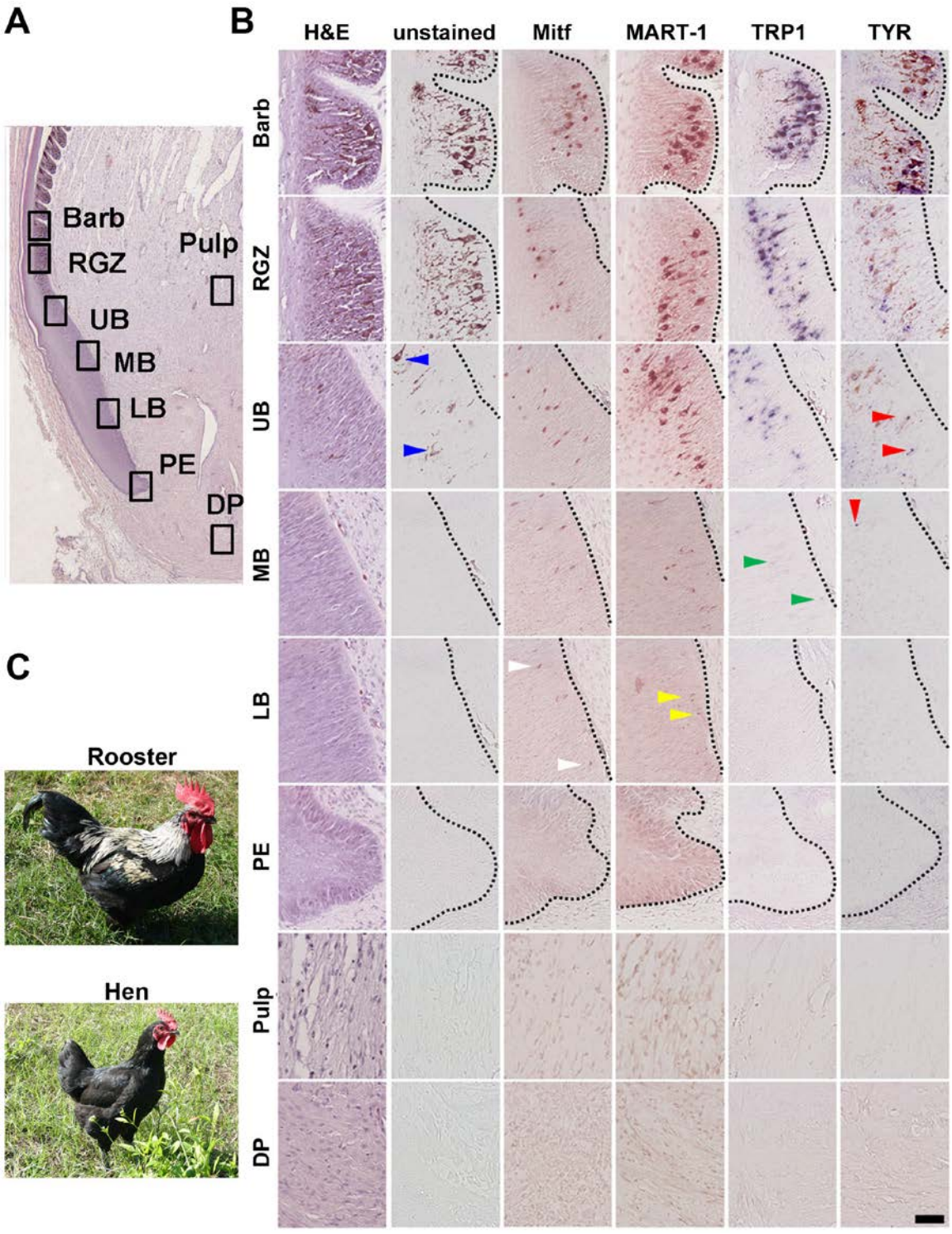


**Melanocyte distribution and differentiation in growing flight feathers of the Black-feathered Taiwan Country Chicken.**

Mitf and MART-1 were detected by immunohistochemistry. TRP1 and TYR were detected by *in situ* hybridization. For better view of Mitf, MART-1, TRP1 and TYR expression, the melanin was bleached after color development for immunohistochemistry or *in situ* hybridization. Bar: 50μm

A. H&E staining. Anatomy of a growing flight feather: dermal papilla (DP), pulp, papilla ectoderm (PE), lower bulge (LB), middle bulge (MB), upper bulge (UB), ramogenic zone (RGZ), and barb.
B. Pigment, distribution, and differentiation of melanocytes. Magnified micrographs from the corresponding boxed areas in panel A. Small apigmented melanocytes with weak staining for Mitf (white arrowheads) and MART-1 (yellow arrowheads) were present in LB. The intensity of Mitf and MART-1 staining progressively increased upwards toward the barbs. TRP1 expression was first detected (green arrowheads) in MB and the expression progressively increased towards the barbs. TYR expression was first detected at the junction of MB and UB (red arrowheads), and the expression level progressively increased upwards. Unstained sections showed that the melanin pigment first appeared in UB (blue arrowheads) and the amount of pigment increased toward the barbs. No melanocytes were revealed in the pulp, dermal papilla or epithelium of the follicular wall. Black dashed line: epithelial-mesenchymal junction. Bar: 50μm.
C. Adult Black-feathered Taiwan Country chickens.

**Fig. S3**

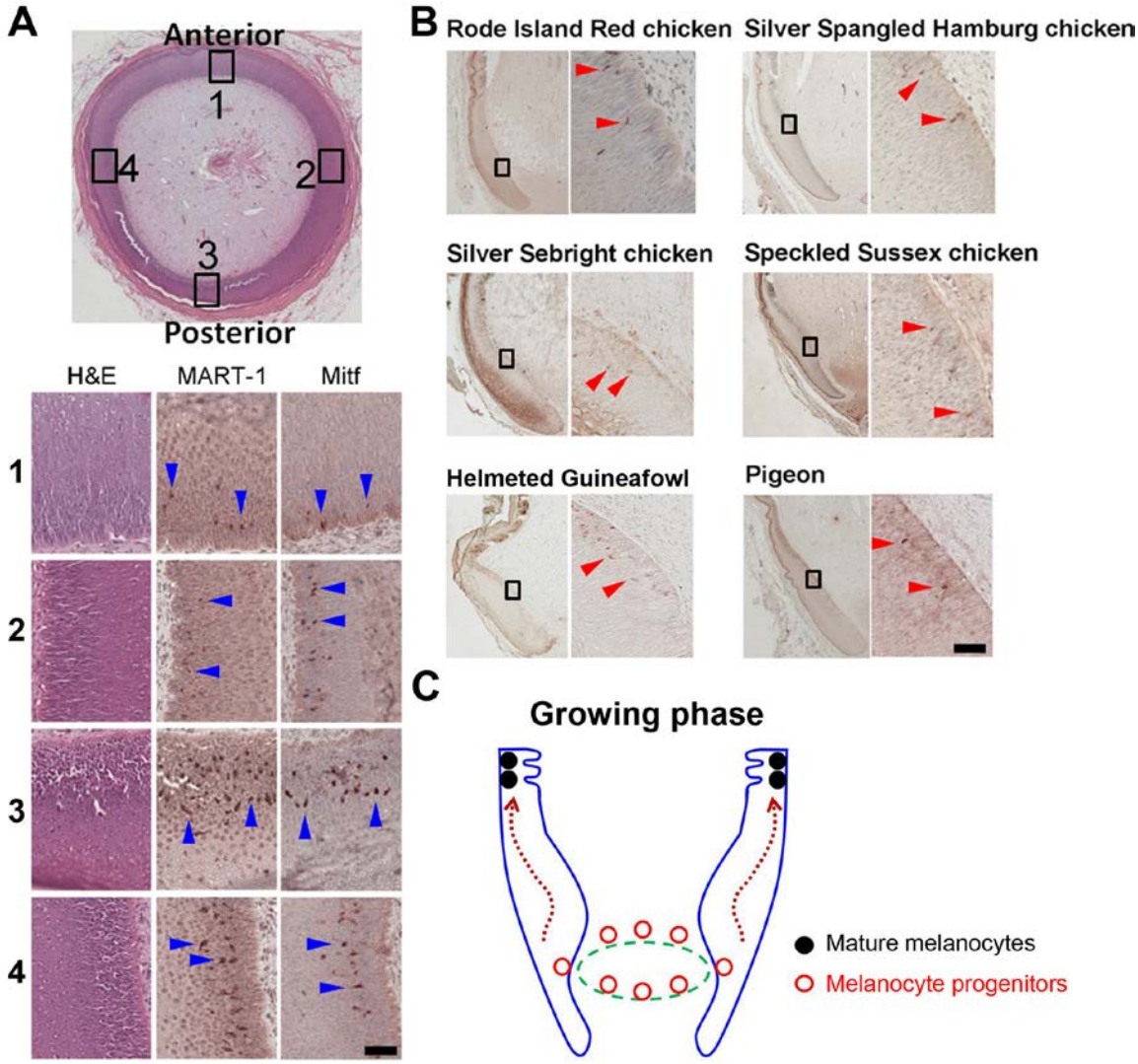


**Distribution of melanocyte progenitors in the lower bulge epithelium in different chicken breeds and non-Gallus birds.**

A. Horizontal section at the lower bulge level of a growing flight feather from a Black-feathered Taiwan Country chicken (upper panel, H&E). The lower panel shows the magnified micrographs of the corresponding boxed areas in the upper panel. $Mitf^{+}$ $MART\text{-}1^{+}$ apigmented melanocytes were found all around the epithelium (blue arrowheads). Bar: 50μm.
B. Mitf staining for apigmented melanocyte progenitors in other chicken breeds and non-Gallus birds. In each bird, the magnified micrograph shows the corresponding boxed area in the low-power micrograph. $Mitf^{+}$ apigmented melanocytes (red arrowheads) were present in the lower bulge epithelium of different chicken breeds and non-Gallus birds. Bar: 50μm.

C. Depiction of melanocyte progenitor cell arrangement in the growing feather. The melanocyte progenitors in the lower bulge epithelium are arranged as a horizontal ring surrounding the feather follicle. They send out differentiating progeny upwards to the feather barbs. Dashed arrows indicate direction of cell movement.

**Fig. S4**

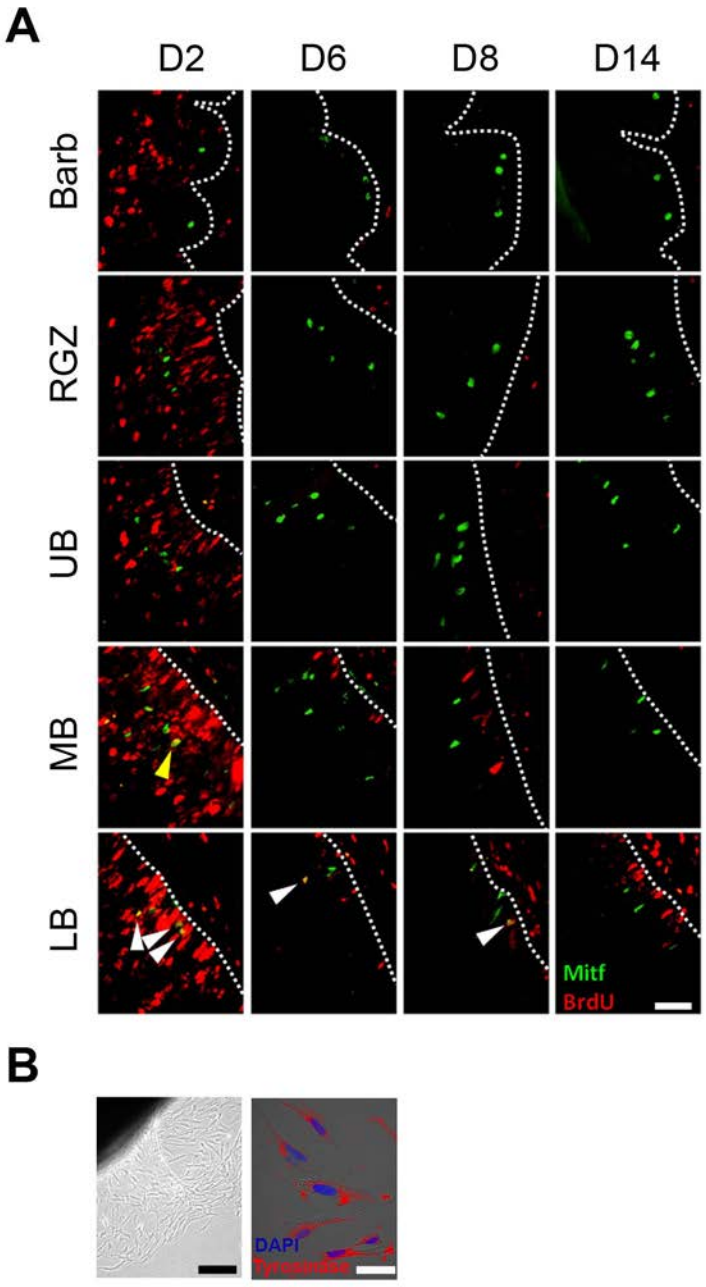


**Melanocyte proliferation status *in vivo* and expression of tyrosinase activity of melanocyte progenitors *in vitro*.**

A. This panel shows the results from regenerating feathers labeled by BrdU in the early growing period (0-14 days after plucking). Melanocytes in the lower bulge retained BrdU (white arrowheads) for 8 days. Above the lower bulge, BrdU could only be retained by melanocytes for up to 2 days in the middle bulge (yellow arrowheads). After 14 days of tracing, only some of the keratinocytes in the lower bulge still

retained BrdU. Regenerating feathers labeled in the middle (15-28 days after plucking) and late (29-42 days after plucking) period of the growing phase showed similar results of BrdU retention in melanocytes. White dashed line: epithelial-mesenchymal junction. Bar: 50μm.

B. Melanocytes could be cultured from explants of the lower bulge region (left panel, phase contrast, 10 days in culture). Under the stimulation of α-MSH for 7 days, melanocytes from the explants displayed tyrosinase activity (right panel, overlay image of bright field and fluorescence). Bar: 100μm in left panel, 25μm in right panel.

**Fig. S5**

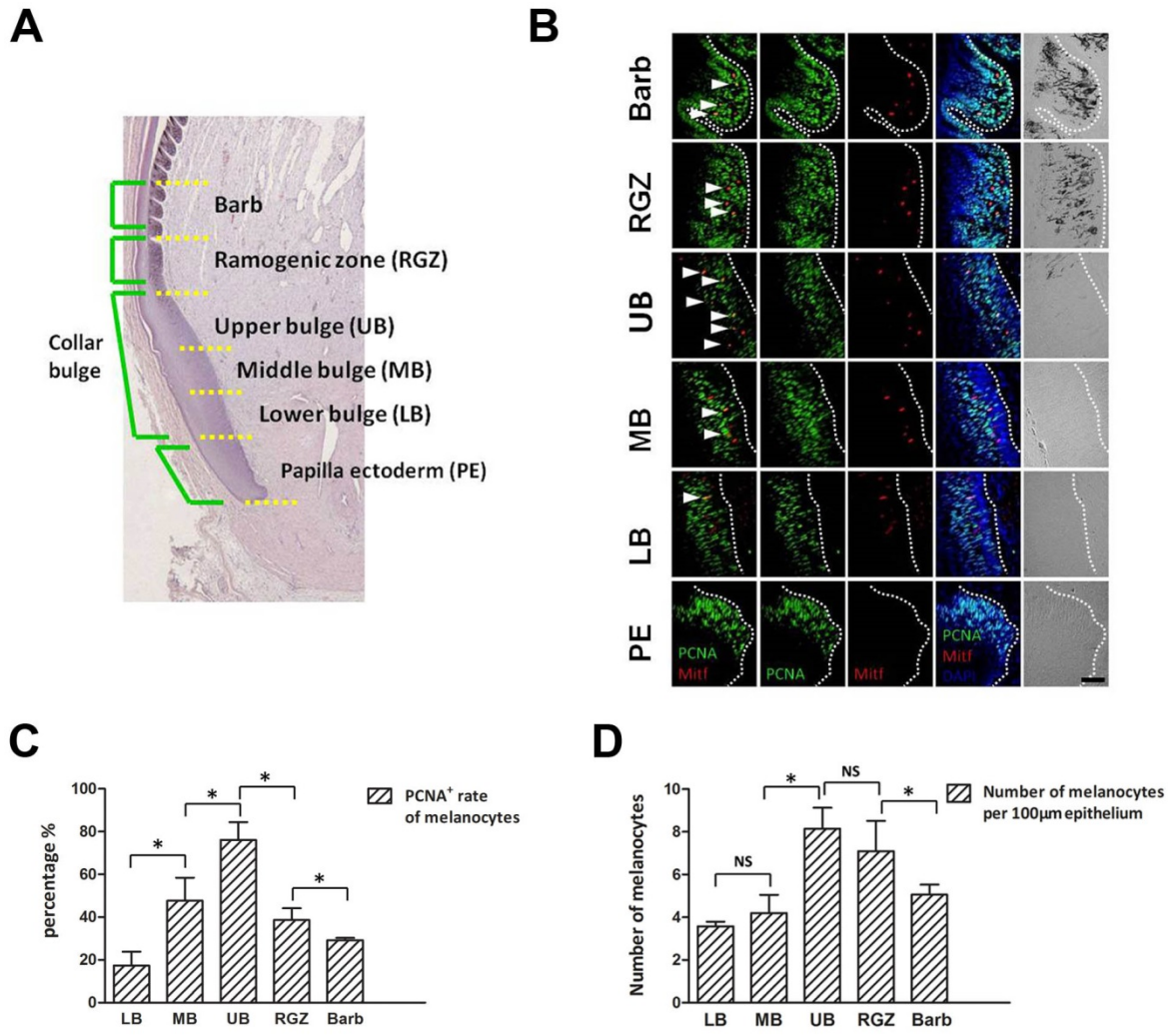


**Melanocyte proliferation status determined by PCNA expression and cell density.**

A. Depiction of the epithelial regions for analysis in growing flight feathers.
B. Immunostaining for PCNA and Mitf. Double positive cells (white arrowheads) were proliferating melanocytes. The rightmost row is the bright field image and white dashed lines represent the epidermal-mesenchymal junction. Bar: 50μm.
C. Quantitative analysis of PCNA positive rates of melanocytes in different regions. Ratio of No. of $PCNA^+$ melanocytes/No. of total melanocytes in each epithelial region was calculated. Apigmented melanocytes in the lower bulge had the lowest rate of PCNA expression. Melanocytes in the middle bulge and upper bulge regions showed a higher percentage of PCNA expression. * $P<0.05$. (N=3)
D. Quantitative analysis of cell density of melanocyte lineage in different regions. Number of Mitf positive cells was calculated in each region. The result was expressed as No. of melanocytes per unit length (100μm) of epithelium. Melanocyte density was

lowest in LB and MB and highest in UB and RGZ. * $P<0.05$; NS: non-significant. (N=3)

**Fig. S6**

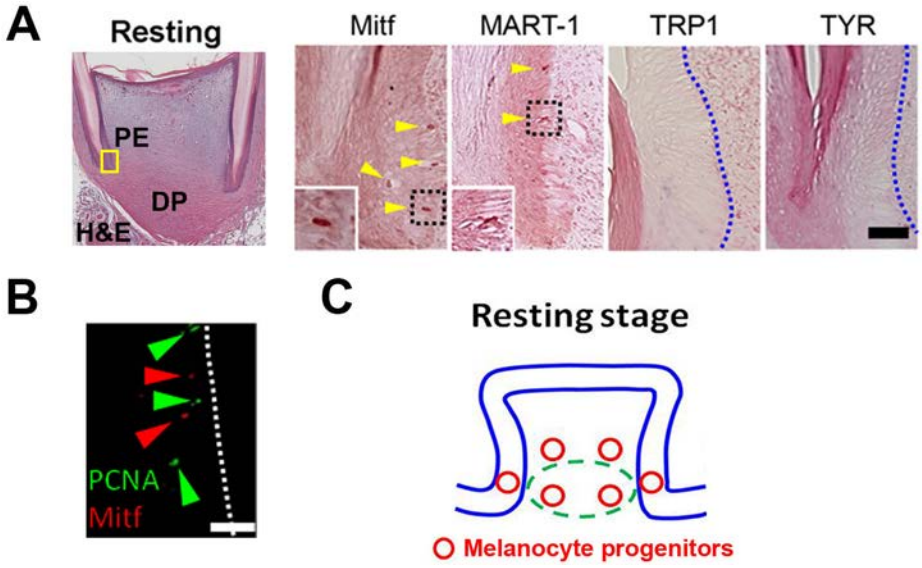


**Distribution of melanocyte progenitors and expression of differentiation and proliferation markers in the resting phase.**

A. The leftmost panel shows the histology (H&E) of a resting follicle. $Mitf^{+}$ $MART\text{-}1^{+}$ apigmented melanocytes (yellow arrowheads) were revealed in the lower tip of the feather epithelium, the papilla ectoderm. They were negative for the differentiation markers, TRP1 and TYR. Right panels were magnified images from the yellow box of the histology. Blue dashed line is epithelial-mesenchymal junction. PE: papilla ectoderm; DP: dermal papilla. Bar: 50μm.
B. PCNA expression in melanocyte progenitors. The $Mitf^{+}$ melanocyte progenitors were negative for PCNA expression in the resting phase (red arrowheads). Only a limited number of keratinocytes were positive for PCNA expression (green arrowheads). White dashed line is epithelial-mesenchymal junction. Bar: 50μm.
C. Depiction of the arrangement of melanocyte progenitors in the resting phase. Compared with the growing phase, the melanocyte progenitors descend to the papilla ectoderm in the resting phase. They are still arranged as a horizontal ring configuration surrounding the feather follicle, but become quiescent.

**Fig. S7**

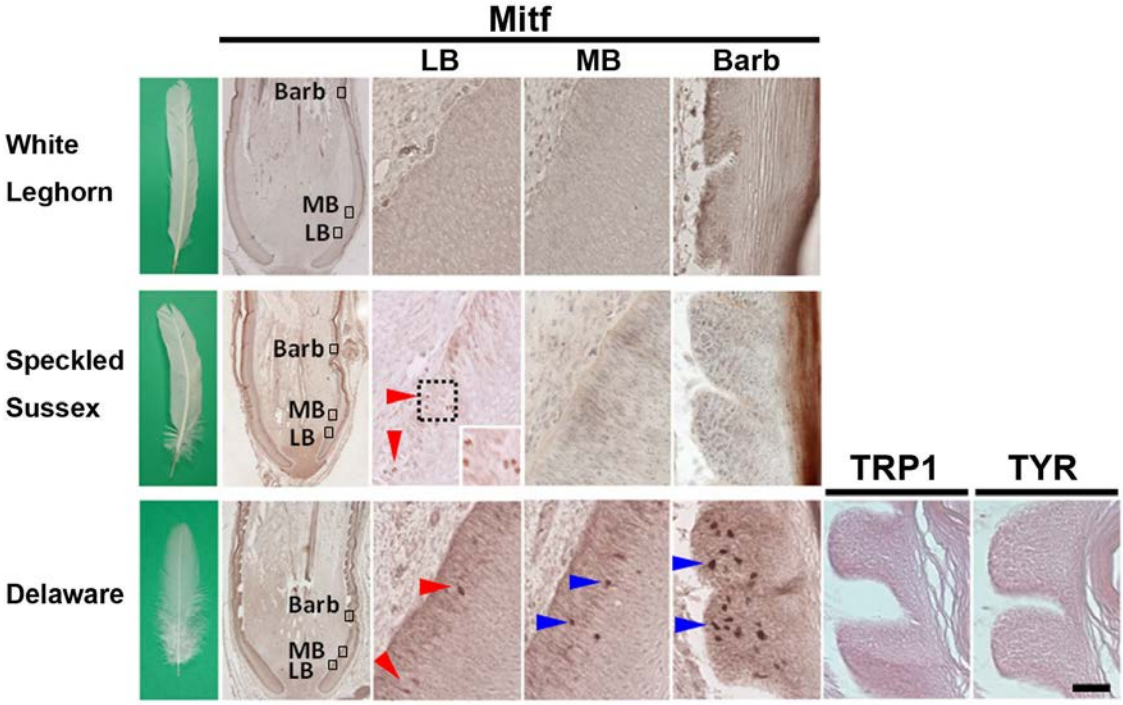


**Distribution of melanocytes and melanocyte progenitors in completely apigmented feathers from White Leghorn, Speckled Sussex, and Delaware chickens.**

Completely apigmented feathers from chicken breeds with different genetic backgrounds are shown. Feather color patterns are displayed on the left row (White Leghorn, Speckled Sussex and Delaware chickens). Growing feather follicles from each breed were stained for Mitf to identify the melanocyte lineage. In apigmented feathers from White Leghorn, the entire melanocyte lineage was absent in the feather. In flight feathers from Speckled Sussex, melanocytes were absent in the epithelium of feather barbs, but melanocyte progenitors were still present in the lower bulge epithelium (red arrowheads and region boxed by the dashed line). In feathers from Delaware, melanocyte progenitors were present in the lower bulge (red arrowheads) and apigmented melanocytes were present from the middle bulge all the way to the barbs (blue arrowheads). The apigmented melanocytes in the barbs were negative for TRP1 and TYR expression. LB: lower bulge; MB: middle bulge. Bar: 50μm

**Fig. S8**

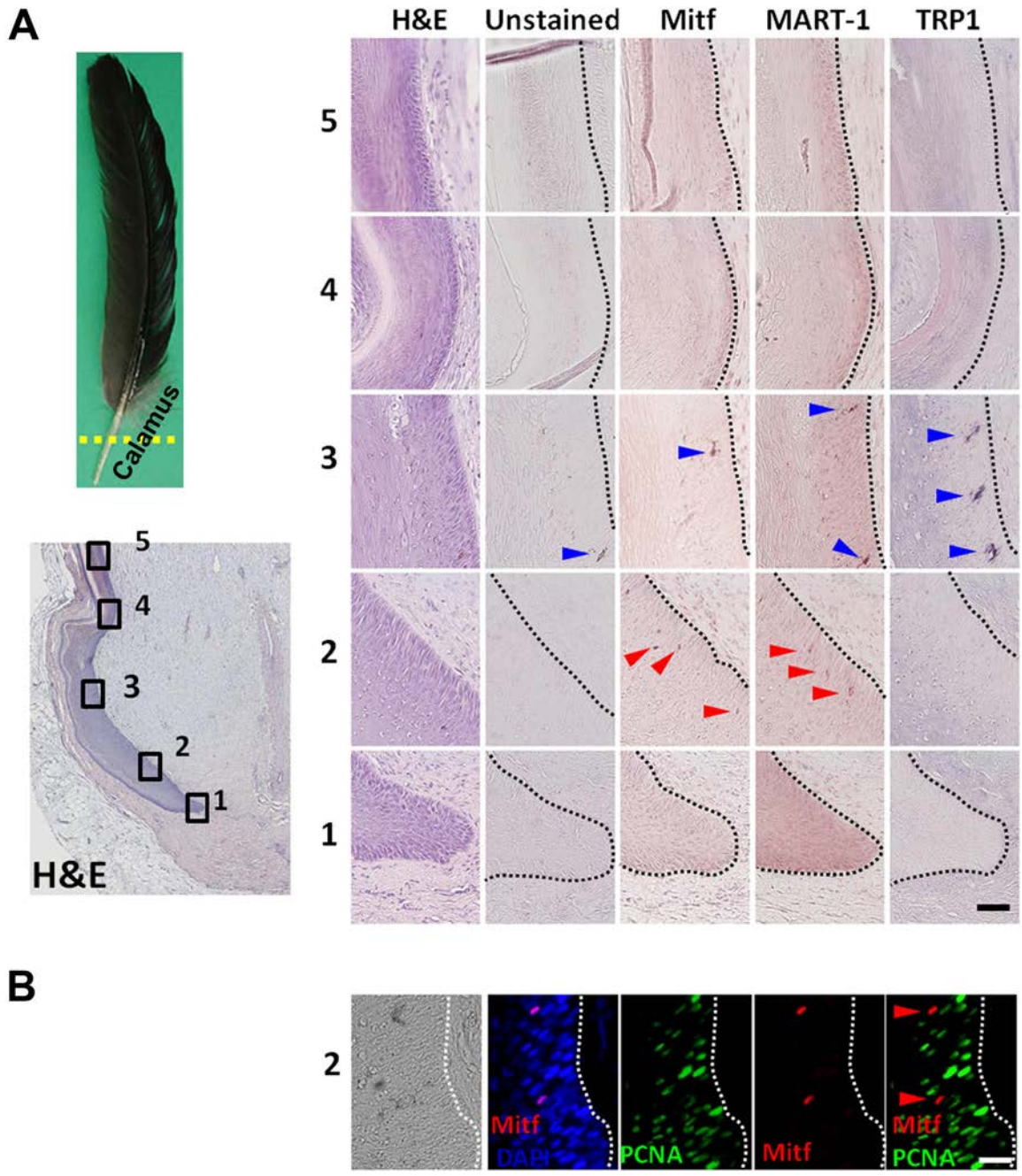


**Distribution and differentiation of melanocytic lineage in the calamus forming stage of the Black-feathered Taiwan Country chicken.**

A. Feather pigment change, histology and expression of melanocyte markers. The yellow dashed line indicates the sampling time point when the apigmented calamus was forming (left upper panel). The right panel shows the magnified micrographs of the

corresponding boxed regions in the left lower panel (H&E). The bulge morphology was lost due to collar shrinkage and there was no barb formation at this stage. H&E and unstained sections showed that the mature calamus epithelium was apigmented and melanocytes were absent (box 4 and box 5). $Mitf^{+}$ $MART\text{-}1^{+}$ $TRP1^{-}$ melanocyte progenitors were present in the lower part of the collar epithelium (red arrowheads, box 2). There were few $Mitf^{+}$ $MART\text{-}1^{+}$ $TRP1^{+}$ pigmented melanocytes located immediately above the progenitor niche (blue arrowheads, box 3). The papilla ectoderm was devoid of melanocytes (box 1). Black dashed line: epithelial-mesenchymal junction. Bar: 50μm;

B. Cell proliferation status. In serial sections, $Mitf^{+}$ melanocyte progenitors in the box 2 region of panel A were negative for PCNA expression (red arrowheads). However, many keratinocytes here were still positive for PCNA expression, indicating that they were still actively proliferating to support calamus elongation. White dashed line: epithelial-mesenchymal junction. Bar: 100μm.

**Fig. S9**

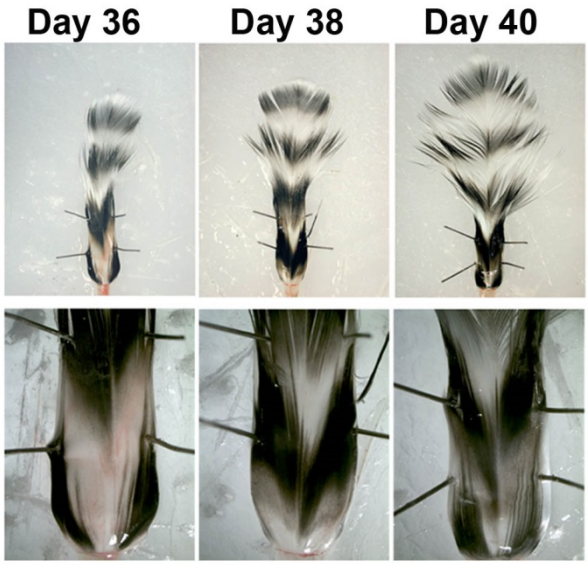


**Dynamic changes of chevron-shaped barring in growing breast feathers of the Barred Plymouth Rock chicken.**

After feather plucking, three adjacent regenerating breast feathers were collected at indicated time points from day 36 to day 40. The mesenchyme was removed and feather epithelium was vertically cut and opened from the posterior side. Alternating chevron-shaped white and black barring was revealed above the ramogenic zone in the opened epithelial cylinder.

There can be quiescent melanocyte progenitors in the posterior part (barb generation zone). These cells come in and travel all the way to the anterior side to replenish the niche. That's how the bars travel toward the anterior side. The ratio of (1. the velocity of progenitor migration toward anterior side) to (2. the velocity of the upward growing of the epithelial cylinder) will determine the angle of the chevron (Fig. 2B, fig. S10D).

The chevron-shaped barring did not become horizontal until the vane was released and opened. The old chevrons moved upwards toward the distal end as the new chevrons formed from the ramogenic zone. The barring pattern on different sides of the rachis could be out of phase and became bilaterally asymmetric.

**Fig. S10**

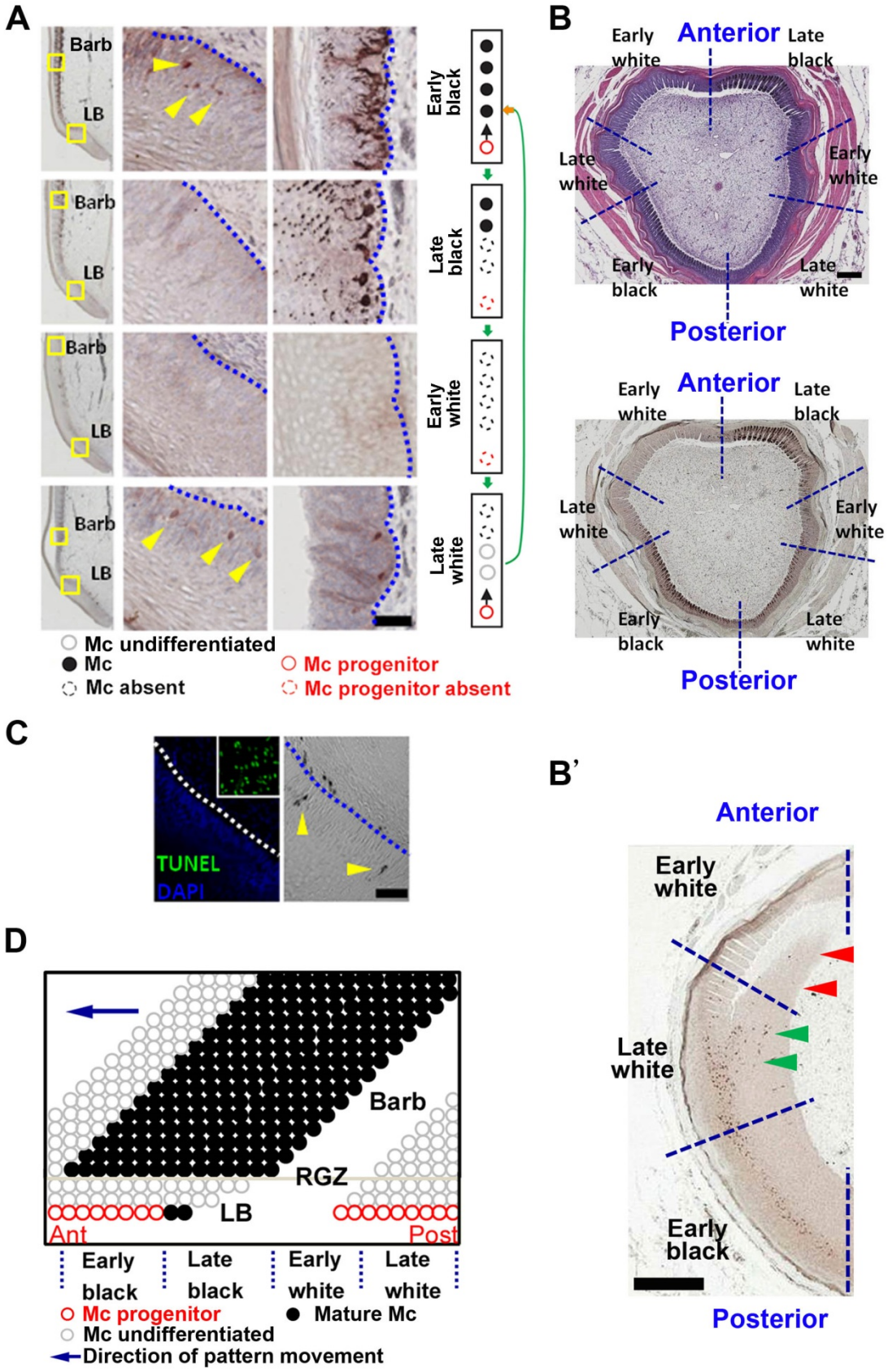
A
Barb
LB
Early black
Late black
Early white
Late white
Mc undifferentiated
Mc
Mc absent
Mc progenitor
Mc progenitor absent
B
Anterior
Posterior
Early white
Late black
Late white
Early black
C
TUNEL
DAPI
B'
D
Barb
RGZ
LB
Ant
Post
Mature Mc
Direction of pattern movement

**Dynamic changes of melanocyte progenitors in McSC niche (lower bulge) in growing breast feathers of the Barred Plymouth Rock chicken.**

We divided the barb pigmentary changes above the ramogenic zone into four sequential phases: early black, late black, early white and late white.

A. Both melanocytes and melanocyte progenitors (yellow arrowheads) were present in early black phase. Melanocyte progenitors disappeared before the barbs turned white in late black phase. In early white phase, both melanocyte progenitors and mature melanocytes were absent. Before pigment regenerated in the barb ridges, melanocyte progenitors appeared in the lower bulge again (yellow arrowheads, late white phase). At this phase, the barb ridges contained undifferentiated melanocytes. The right panel depicts the corresponding cell dynamics. Blue dashed line: epithelial-mesenchymal junction. Bar: 50μm
B. Horizontal sections at barbs right above the ramogenic zone. Upper panel is H&E and lower panel is MART-1 staining. In H&E, the pigmented pattern was not symmetric across the rachis, and all the four phases of pigmentary change could be seen in this horizontal section. Pigmented melanocytes were present in the barb ridges of early and late black regions. No melanocytes were revealed in barb ridges of the early white region, but apigmented melanocytes could be seen in the barb ridges of the late white region. Bar: 250μm.
B'. Horizontal section at the bulge level of the same feather shown in panel B, Mitf staining. Melanocyte progenitors were absent in the anterior side (red arrowheads). There was a band of melanocyte progenitors extending from the posterior side toward the anterior side. Near the anterior end of this progenitor band, sparse dispersed melanocyte progenitors penetrated toward the anterior side (green arrowheads). Bar: 500μm.
C. No apoptosis was detected in the lower bulge by TUNEL assay (left panel; inset was positive control), whereas the bright field image showed premature production of melanin (yellow arrowheads, right panel). Blue or white dashed line: epithelial-mesenchymal junction. Bar: 65μm
D. Depiction of cell dynamics and pattern movement in chevron-shaped barring. The pigment pattern right above the RGZ is divided into 4 regions: early black, late black, early white and late white. Above the RGZ, pigmented melanocytes are present in early and late black, and become absent in early white. In late white, melanocytes reappear in the barbs, but are apigmented. In the LB niche, melanocyte progenitors are present in early black. Premature differentiation of melanocyte progenitors leads to progenitor cell depletion in late black and the niche remains empty in early white. Melanocyte progenitors, presumably coming from the remaining melanocyte progenitors on the posterior side, reappear in the LB in late white. As feathers continue to grow, this alternating black and white chevron-shaped barring pattern moves from the posterior side to the anterior side. The local melanocyte progenitors in the LB are repeatedly depleted and replenished, creating the cyclic barring pattern. LB: lower bulge; RGZ: ramogenic zone; ant: anterior; post: posterior.

**Fig. S11**

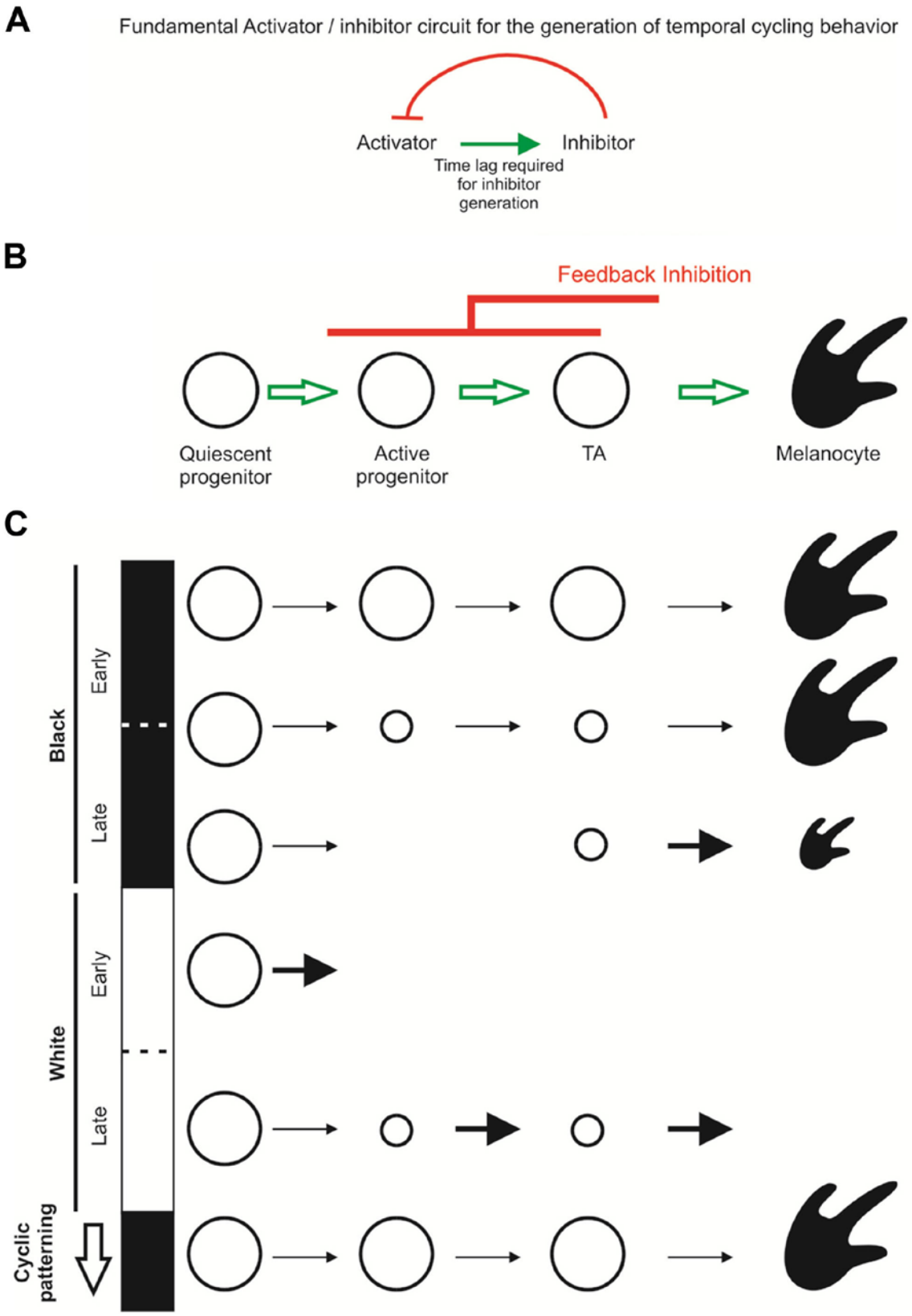
A
Fundamental Activator / inhibitor circuit for the generation of temporal cycling behavior
Activator
Inhibitor
Time lag required for inhibitor generation
B
Feedback Inhibition
Quiescent progenitor
Active progenitor
TA
Melanocyte
C
Black
Early
Late
White
Early
Late
Cyclic patterning

**A. Fundamental model for cyclic behavior**

An activator stimulates the production of an inhibitor, but there is a time lag between its induction and appearance. The inhibitor then inhibits the activator, providing for cyclic behavior.

**B. Hypothetical model to generate a feedback loop during melanocyte differentiation, thus temporally periodic pattern**

Inhibitors produced from the activation of progenitors can prevent quiescent progenitors from becoming activated, or activated progenitor cells from becoming TA cells, or TA cells from differentiating or the self-renewal of progenitors. During melanocyte progression, we envision a model of feedback inhibition, although the source of the inhibitor and the level at which it functions have yet to be determined. In Barred Plymouth Rock chickens, there is feedback inhibition when melanocyte progenitors are activated. This inhibition removes progenitors by promoting their differentiation. TA: transit amplifying cell.

**C. Hypothetical model to generate stripes based on the current experimental data**

In Barred Plymouth Rock chickens, inhibitors are aberrantly expressed when progenitors are activated due to gain-of-function mutation involving CDKN2A/B locus that encodes tumor suppressor genes *INK4b* and *ARF* (*14*). Therefore, toward the second half of the black bar, the number of activated progenitors decrease (symbol size indicates population size, not cell size). Eventually activated melanocyte progenitors are exhausted, forming the early half of the white bar. Quiescent melanocyte progenitors then replenish activated melanocyte progenitors (late white region), which reconstitutes the homeostasis and black bar (early black region). Due to the reappearance of the inhibitor upon progenitor activation, activated melanocyte progenitors will exhaust themselves again, forming the white bar.

**Fig. S12**

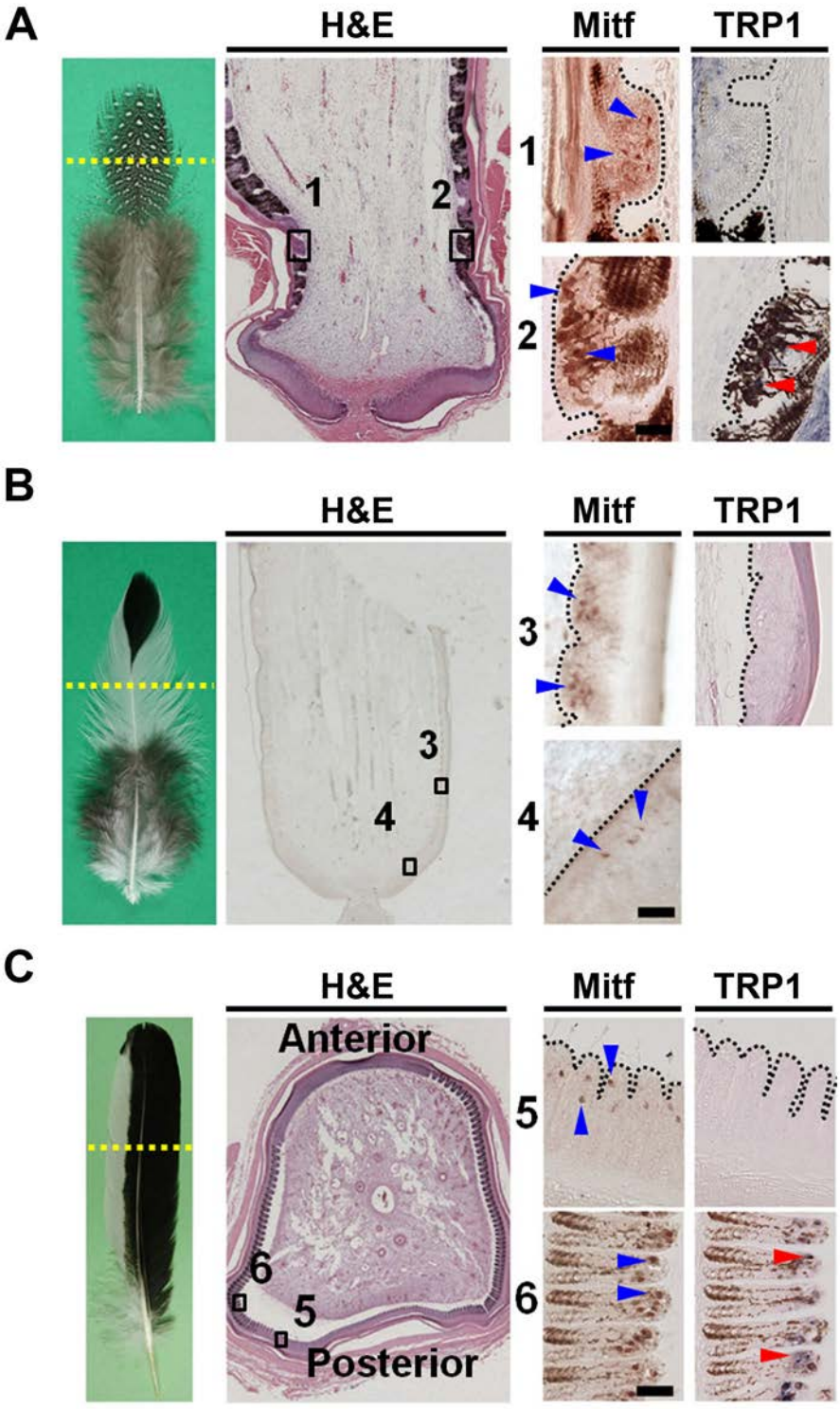


**Distribution of melanocytes and melanocyte progenitors in feathers from Helmeted Guineafowl, Silver Spangled Hamburg chicken and Silver Laced Wyandotte chicken.**

The data show patterned apigmented regions in these feathers are due to suppressed melanocyte differentiation. Dashed lines on the gross feather appearance indicate the time point when the growing feather was removed for histological examination. Micrographs on the right side show magnified views of the corresponding boxed region in the low-power view on the left. Black dashed line: epithelial-mesenchymal junction. Bar: 50μm.

A. **Saddle feather from a Helmeted Guineafowl**. Vertical sections show that $Mitf^{+}$ melanocytes were present both in the apigmented (blue arrowheads, box 1) and pigmented (blue arrowheads, box 2) barb ridges. The pigmented melanocytes were positive for TRP1 expression (red arrowheads, box 2), while apigmented melanocytes were negative for this differentiation marker.
B. **Breast feather from a Silver Spangled Hamburg chicken**. Melanocyte progenitors were present in the lower collar bulge (blue arrowheads, box 4). In the apigmented barb ridges, $Mitf^{+}$ melanocytes were present (blue arrowheads, box 3), but they were negative for the TRP1 differentiation marker.
C. **Flight feather from a Silver Laced Wyandotte chicken**. Horizontal sections just above the ramogenic zone showed that $Mitf^{+}$ melanocytes were present both in the pigmented (blue arrowheads, box 6) and apigmented (blue arrowheads, box 5) barb ridges. However, only pigmented melanocytes were positive for TRP1 expression (red arrowheads, box 6).

**Fig. S13**

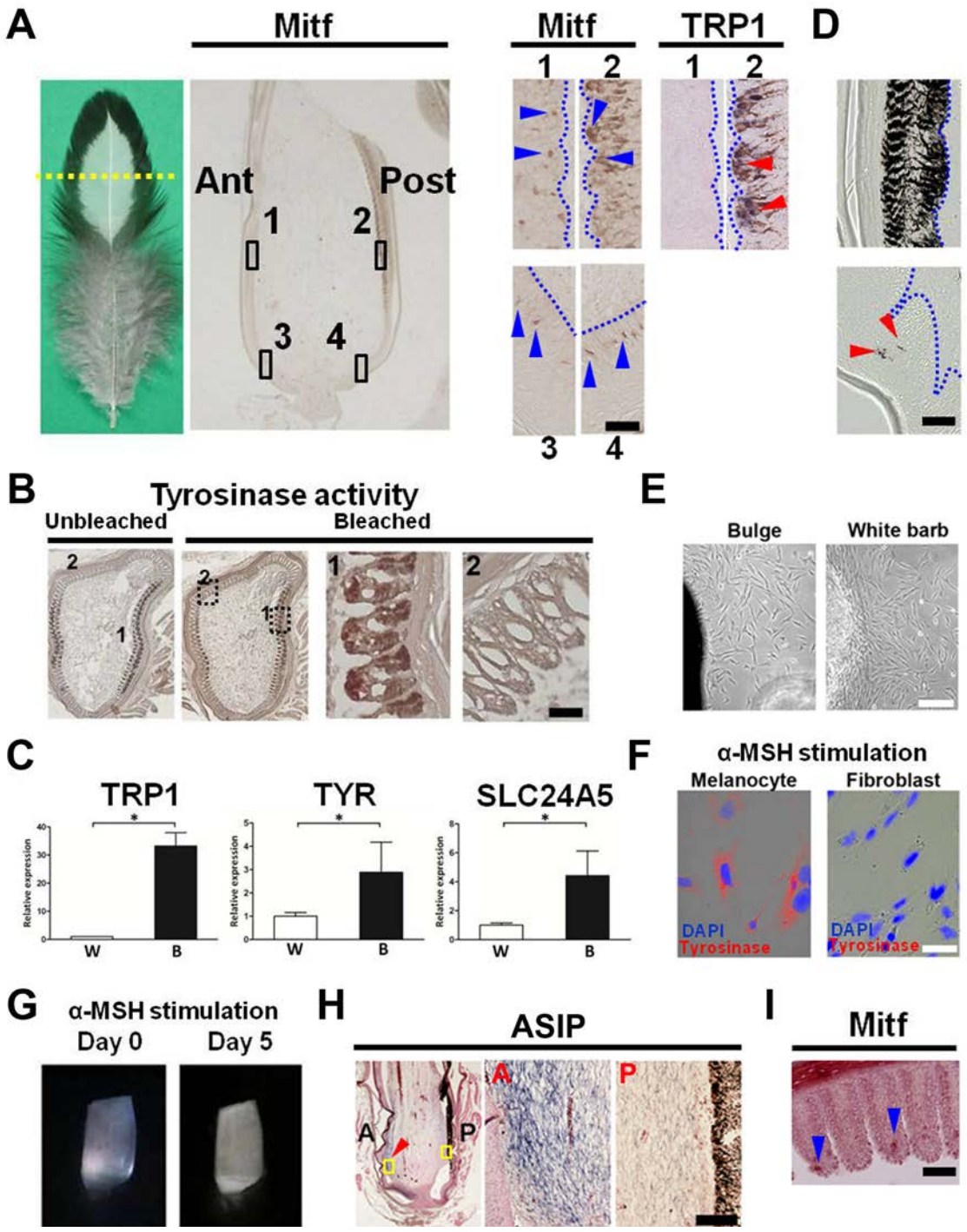


**Apigmented barb regions are due to suppressed melanocyte differentiation in Silver Laced Wyandotte chicken feathers.**

A. At the early growing period (about 14 days after feather plucking) when the single

black lace was forming (dashed line, left panel), feather follicles were collected for analysis. In the vertical section, the anterior side (Ant) was apigmented and the posterior side (Post) was pigmented. $Mitf^{+}$ melanocyte progenitors were present in the lower bulge epithelium (blue arrowheads, box 3 and box 4, Mitf staining) of both sides. Melanocytes were also present in the barb ridges of both sides (blue arrowheads, box 1 and box 2, Mitf staining). However, melanocytes in the apigmented barb ridges were negative for TRP1 expression (box 1, TRP1), while pigmented melanocytes in the pigmented barb ridges were positive for TRP1 expression (red arrowheads, box 2, TRP1). Micrographs on the right side show magnified views of the corresponding boxed region in the low-power view on the left. Blue dashed line: epithelial-mesenchymal junction. Bar: 50μm.

B. Tyrosinase activity determined by tyramide reaction. For a better view of tyrosinase activity, the specimen was bleached to remove melanin color after color development. Melanocytes in the pigmented barb ridges (box 1) were positive for tyrosinase activity while melanocytes in the apigmented barb ridges (box 2) were negative for tyrosinase activity. Bar: 50μm.
C. Real-time PCR for quantification of gene expression level. Compared with the black pigmented region (B), differentiation markers of melanocytes including TRP1, TRY and SLC24A5 were all significantly downregulated in the white apigmented region (W). * $p<0.05$. (N=3).
D. Unstained sections of the pigmented (upper panel) and apigmented barbs (lower panel). Pigmented melanocytes could occasionally be observed in the apigmented barb ridges (red arrowheads). Blue dashed line: epithelial-mesenchymal junction. Bar: 50μm.
E. Melanocytes could be cultured from both the white barbs and the bulge of the feather shown in panel A. Bar: 100μm.
F. Under α–MSH (2.5 μg/ml) stimulation, melanocytes isolated from white barbs acquired tyrosinase activity. Bar: 25μm.
G. *In vitro* stimulation with α–MSH. Apigmented feather explants containing both the epithelium and adjacent pulp mesenchyme were stimulated with α–MSH (2.5 μg/ml) for 7 days. The explants remained apigmented in the presence of α–MSH (N=8).
H. In *situ hybridization* to detect ASIP expression in the feather section. In this feather, the anterior side was apigmented and the posterior side was pigmented. The leftmost panel showed the low-power view (A: anterior side; P: posterior side). The middle and rightmost panel were enlarged micrographs of the boxed areas in the low-power view. Peripheral pulp cells on the apigmented side exhibited higher ASIP expression (red arrowhead). Bar: 100μm.
I. Feather follicles treated with ASIP-coated beads. $Mitf^{+}$ melanocytes were still present in the barbs (blue arrowheads), but they did not produce melanin pigment. Bar: 50μm.

**Fig. S14**

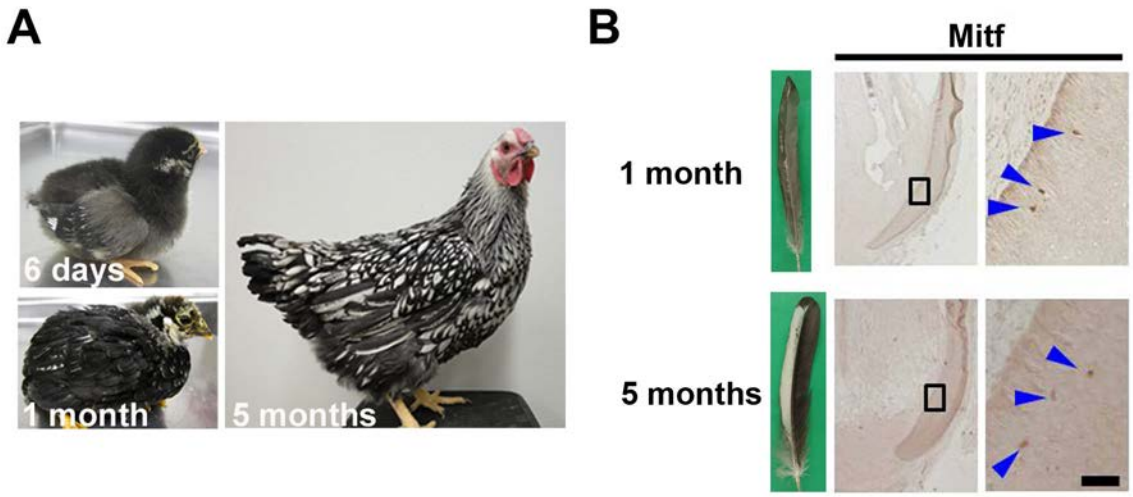


**Age-related pigment pattern change and location of melanocyte progenitors.**

A. Change of plumage color with age in a female Silver Laced Wyandotte chicken.

B. Age-related pigment pattern change and the location of melanocyte progenitors in the same feather follicle at different ages. Though the pigment pattern of feathers from the right 4th secondary flight feather of Silver Laced Wyandotte chickens differed at 1 and 5 months of age (leftmost panels), the distribution of melanocyte progenitors in the lower bulge of the growing feather follicle was similar (blue arrowheads). Rightmost panels were the magnified image of the corresponding boxed areas. Bars: 50μm.

**Fig. S15**

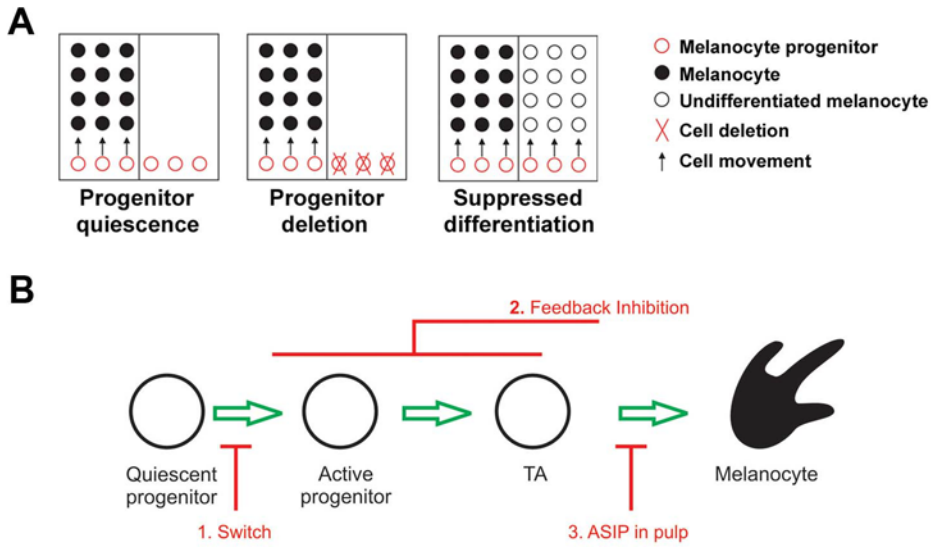


**Cellular mechanisms and regulation for pigment patterning.**

**A. Different cellular mechanism for apigmentation formation in feathers.** Apigmentation can be caused by premature progenitor quiescence entry, deletion of progenitors in the niche and suppressed differentiation. The rectangle represents an opened feather cylinder, like that seen in Fig. 4B.

**B. A generic model for homeostasis of melanocyte stem cell progression**.

There are many possible steps to modulate the homeostasis of melanocyte stem cells and thus generate pigment pattern formation. The modulation can be based on auto-feedback or cross-talk with environments such as the peripheral pulp or body hormone status. Three examples based on the data are shown here. We expect more molecules to be found, particularly those based on the rich source of avian genetic breeds with complex plumage patterns. We expect the site of those gene actions to be mapped on this simple progressive pathway, which in turn is regulated in the multi-dimensional space we depicted in Fig. 4B to generate complex pigment patterns.

**References**


1. C. M. Chuong, V. A. Randall, R. B. Widelitz, P. Wu, T. X. Jiang, Physiological regeneration of skin appendages and implications for regenerative medicine. *Physiology* **27**, 61 (2012). doi:10.1152/physiol.00028.2011 Medline

2. G. E. Hill, K. J. McGraw, *Bird Coloration* , G. E. Hill, K. J. McGraw, Eds. (Harvard University Press, Cambridge, Massachusetts, 2006).

3. A. M. Lucas, P. R. Stettenheim, *Avian Anatomy: Integument. Agriculture Handbook 362: Agricultural Research Service*. (U.S. Department of Agriculture, Washington DC, 1972), vol. 2.

4. M. Yu *et al*., The biology of feather follicles. *Int. J. Dev. Biol.* **48**, 181 (2004). doi:10.1387/ijdb.15272383 Medline

5. C. Darwin, *On the Origins of Species by Means of Natural Selection* (John Murray, London, 1859).

6. F. Zhang *et al*., Fossilized melanosomes and the colour of Cretaceous dinosaurs and birds. *Nature* **463**, 1075 (2010). doi:10.1038/nature08740 Medline

7. Q. Li *et al*., Plumage color patterns of an extinct dinosaur. *Science* **327**, 1369 (2010). doi:10.1126/science.1186290 Medline

8. E. Dupin, N. M. Le Douarin, Development of melanocyte precursors from the vertebrate neural crest. *Oncogene* **22**, 3016 (2003). doi:10.1038/sj.onc.1206460 Medline

9. Z. Yue, T. X. Jiang, R. B. Widelitz, C. M. Chuong, Mapping stem cell activities in the feather follicle. *Nature* **438**, 1026 (2005). doi:10.1038/nature04222 Medline

10. E. K. Nishimura *et al*., Dominant role of the niche in melanocyte stem-cell fate determination. *Nature* **416**, 854 (2002). doi:10.1038/416854a Medline

11. P. Rabbani *et al*., Coordinated activation of Wnt in epithelial and melanocyte stem cells initiates pigmented hair regeneration. *Cell* **145**, 941 (2011). doi:10.1016/j.cell.2011.05.004 Medline

12. P. Stettenheim, A light account of plumes. *Science* **333**, 939 (2011). doi:10.1126/science.1209682

13. G. Montalenti, A physiological analysis of the barred pattern in Plymouth Rock feathers. *J. Exp. Zool.* **69**, 269 (1934). doi:10.1002/jez.1400690205

14. A. R. Hellström *et al*., Sex-linked barring in chickens is controlled by the CDKN2A /B tumour suppressor locus. *Pigment Cell Melanoma Res.* **23**, 521 (2010). doi:10.1111/j.1755-148X.2010.00700.x

15. G. S. Barsh, The genetics of pigmentation: From fancy genes to complex traits. *Trends Genet.* **12**, 299 (1996). doi:10.1016/0168-9525(96)10031-7 Medline

16. M. M. Ollmann, M. L. Lamoreux, B. D. Wilson, G. S. Barsh, Interaction of Agouti protein with the melanocortin 1 receptor in vitro and in vivo. *Genes Dev.* **12**, 316 (1998). doi:10.1101/gad.12.3.316 Medline

17. S. E. Millar, M. W. Miller, M. E. Stevens, G. S. Barsh, Expression and transgenic studies of the mouse agouti gene provide insight into the mechanisms by which mammalian coat color patterns are generated. *Development* **121**, 3223 (1995). Medline

18. C. R. Linnen, E. P. Kingsley, J. D. Jensen, H. E. Hoekstra, On the origin and spread of an adaptive allele in deer mice. *Science* **325**, 1095 (2009). doi:10.1126/science.1175826 Medline

19. E. Aberdam *et al*., Involvement of microphthalmia in the inhibition of melanocyte lineage differentiation and of melanogenesis by agouti signal protein. *J. Biol. Chem.* **273**, 19560 (1998). doi:10.1074/jbc.273.31.19560 Medline

20. M. Manceau, V. S. Domingues, R. Mallarino, H. E. Hoekstra, The developmental role of Agouti in color pattern evolution. *Science* **331**, 1062 (2011). doi:10.1126/science.1200684 Medline

21. C. Yoshihara *et al*., Elaborate color patterns of individual chicken feathers may be formed by the agouti signaling protein. *Gen. Comp. Endocrinol.* **175**, 495 (2012). doi:10.1016/j.ygcen.2011.12.009 Medline

22. Y. Yamaguchi, V. J. Hearing, Physiological factors that regulate skin pigmentation. *Biofactors* **35**, 193 (2009). doi:10.1002/biof.29 Medline

23. S. Kondo, T. Miura, Reaction-diffusion model as a framework for understanding biological pattern formation. *Science* **329**, 1616 (2010). doi:10.1126/science.1179047 Medline

24. R. O. Prum, S. Williamson, Reaction-diffusion models of within-feather pigmentation patterning. *Proc. Biol. Sci.* **269**, 781 (2002). doi:10.1098/rspb.2001.1896 Medline

25. F. Lillie, H. Wang, Physiology and development of the feather. V. Experimental morphogenesis. *Physiol. Zool.* **14**, 103 (1941).

26. Y. Yamaguchi *et al*., Mesenchymal-epithelial interactions in the skin: increased expression of dickkopf1 by palmoplantar fibroblasts inhibits melanocyte growth and differentiation. *J. Cell Biol.* **165**, 275 (2004). doi:10.1083/jcb.200311122 Medline

27. C. M. Chuong, M. K. Richardson, Pattern formation today. *Int. J. Dev. Biol.* **53**, 653 (2009). doi:10.1387/ijdb.082594cc Medline

28. S. J. Lin *et al*., Feather regeneration as a model for organogenesis. *Dev. Growth Differ.* **55**, 139 (2013). doi:10.1111/dgd.12024 Medline

29. G. Coquerelle, *Les Poules: Diversité Génétique Visible* (L'Institut National de la Recherche Agronomique, Paris, 2000).

30. B. Reeder, *An Introduction to Color Forms of the Domestic Fowl* (AuthorHouse, Bloomington, Indiana, 2006).

31. C. H. Chao *et al*., The growth performances of commercial red-feathered and black-feathered Taiwan Country Chicken. *J. Chin. Soc. Anim. Sci.* **34**, 65 (2005).

32. Z. Yue, T. X. Jiang, R. B. Widelitz, C. M. Chuong, Wnt3a gradient converts radial to bilateral feather symmetry via topological arrangement of epithelia. *Proc. Natl. Acad. Sci. U.S.A.* **103**, 951 (2006). doi:10.1073/pnas.0506894103 Medline

33. M. Yu, P. Wu, R. B. Widelitz, C. M. Chuong, The morphogenesis of feathers. *Nature* **420**, 308 (2002). doi:10.1038/nature01196 Medline

34. W. Korytowski, T. Sarna, Bleaching of melanin pigments. Role of copper ions and hydrogen peroxide in autooxidation and photooxidation of synthetic dopa-melanin. *J. Biol. Chem.* **265**, 12410 (1990). Medline

35. R. Han, H. P. Baden, J. L. Brissette, L. Weiner, Redefining the skin's pigmentary system with a novel tyrosinase assay. *Pigment Cell Res.* **15**, 290 (2002). doi:10.1034/j.1600-0749.2002.02027.x Medline

36. C. S. Ng *et al*., The chicken frizzle feather is due to an α-keratin (KRT75) mutation that causes a defective rachis. *PLoS Genet.* **8**, e1002748 (2012). doi:10.1371/journal.pgen.1002748 Medline

37. R. R. Bowers, J. E. Gatlin, A simple method for the establishment of tissue culture melanocytes from regenerating fowl feathers. *In Vitro Cell. Dev. Biol.* **21**, 39 (1985). doi:10.1007/BF02620912 Medline

38. C. M. Yen, C. C. Chan, S. J. Lin, High-throughput reconstitution of epithelial-mesenchymal interaction in folliculoid microtissues by biomaterial-facilitated self-assembly of dissociated heterotypic adult cells. *Biomaterials* **31**, 4341 (2010). doi:10.1016/j.biomaterials.2010.02.014 Medline